Gut-associated bacteria invade the midgut epithelium of *Aedes aegypti* and stimulate innate immunity and suppress Zika virus infection in cells.

Shivanand Hegde[1,2], Denis Voronin[3], Aitor Casas-Sanchez[1,2] Miguel Saldaña[4], Alvaro Acosta-Serrano[1,2], Vsevolod L. Popov[5], Ashok K. Chopra[4], Grant L. Hughes[1,2#]

[1]Department of Vector Biology, Liverpool School of Tropical Medicine, Liverpool, United Kingdom

[2]Department of Tropical Disease Biology, Liverpool School of Tropical Medicine, Liverpool, United Kingdom

[3]Laboratory of Molecular Parasitology, New York Blood Center, New Yer, NY, USA

[4]Department of Microbiology and Immunology, University of Texas Medical Branch, Galveston, TX, USA,

[5]Department of Pathology, University of Texas Medical Branch, Galveston, TX, USA.

[#]Corresponding author. Grant Hughes: grant.hughes@lstmed.ac.uk

Abstract

Microbiota within mosquitoes influence nutrition, immunity, fecundity, and the capacity to transmit pathogens. Despite their importance, we have a limited understanding of host-microbiota interactions, especially at the cellular level. It is evident bacterial symbionts that are localized within the midgut also infect other organs within the mosquito; however, the route these symbionts take to colonize other tissues is unknown. Here, utilizing the gentamicin protection assay, we showed that the bacterial symbionts *Cedecea neteri* and *Serratia mercescens* have the capacity to invade and reside intracellularly within mosquito cells. Symbiotic bacteria were found within a vacuole and bacterial replication was observed in mosquito cell by transmission electron microscopy, indicating bacteria were adapted to the intracellular milieu. Using gene silencing, we determined that bacteria exploited host factors, including actin and integrin receptors, to actively invade mosquito cells. As microbiota can affect pathogens within mosquitoes, we examined the influence of intracellular symbionts on Zika virus (ZIKV) infection. Mosquito cells harbouring intracellular bacteria had significantly less ZIKV compared to uninfected cells or cells exposed to non-invasive bacteria. Intracellular bacteria were observed to substantially upregulate the Toll and IMD innate immune pathways, providing a possible mechanism mediating these anti-viral effects. Examining mono-axenically infected mosquitoes using transmission electron and fluorescent microscopy revealed that bacteria occupied an intracellular niche *in vivo*. Our results provided evidence that bacteria that associate with the midgut of mosquitoes have intracellular lifestyles which likely have implications for mosquito biology and pathogen infection. This study expands our understanding of host-microbiota interactions in

mosquitoes, which is important as symbiont microbes are being exploited for vector control strategies.

Introduction

Mosquitoes are holometabolous insects with aquatic and terrestrial life stages. Aquatic stages are continually exposed to microbes in the larval habitat while adults likely acquire microbiota from the environment after eclosion or when nectar feeding [1-3]. Additionally, environmentally acquired microbes may persist in mosquito tissues between aquatic and adult life states facilitating transstadial transmission [4-6]. It is likely that these processes contribute to the considerable variability seen in the adult microbiome [7-9]. While our understanding of genetic factors that influence host-microbe interactions and microbiome acquisition are expanding [10, 11], we still have a poor knowledge of these interactions at the cellular level. Given the importance of the microbiome on mosquito traits relevant for vectorial capacity and vector competence [12-15], understanding processes that influence microbiome homeostasis is critical for developing microbial-based control strategies [16, 17].

Bacterial microbiota often resides within several organs in mosquitoes and appears to be able to migrate between tissues. Several studies have identified bacteria in the gut of mosquitoes [9, 18-20], which have led to these microbes being commonly referred to as gut microbes, but many of these bacterial species also colonize other tissues such as the salivary gland [18, 20-23], reproductive tract [20, 22, 24], or malpighian tubules [4]. While some bacteria are unique to each tissue, several infect multiple tissues within the mosquito [20, 25], and localization in organs such as the malpighian tubules and reproductive tissues likely enables transmission between life stages and generations, respectively. Both *Asaia* and *Serratia* are transferred vertically to progeny after

69 administered to the mosquito in a sugar meal, suggesting symbiotic bacteria have the
70 capacity to translocate from the midgut to the germline of their host [20, 26-28].
71 However, mechanisms facilitating their translocation remain elusive. Infection of the
72 entomopathogic fungus *Beavaria* of *Anopheles* mosquitoes enabled *Serratia* to escape
73 the midgut and over replicate in the hemolymph, which was the cause of mortality to the
74 insect [29]. In *Drosophila*, orally infected *Serratia* localized within the midgut epithelium
75 [30]. While the epithelial infection was rare in wild type flies, *Serratia* was observed to
76 localize intracellularly in *imd* knock-out flies, suggesting that host immunity influenced
77 cellular localization or controlled infections [30]. Although intracellular bacterial
78 infections have been observed in the midgut of flies [30], cellularity of gut-associated
79 bacterial infections in mosquitoes and the mechaimism facilitating systemic infection of
80 different tissues is largely unknown. It is plausible that an intracellular lifestyle could
81 provide a mechanism for transstadial and vertical transmission of bacteria in mosquito
82 vectors.
83
84 In mammalian systems, bacteria exploit their invasive capability to colonize host tissue
85 and systemically spread within multicellular organisms [31-33]. Pathogenic bacteria like
86 *Listeria, Salmonella, Vibrio,* and *Yersinia* invade host cells to colonize, replicate, and
87 migrate between cells [32]. While the invasive capacity and mechanisms have been
88 studied extensively in mammalian cells, *in vitro* investigation in mosquitoes or other
89 arthropod vectors is lacking. In order to obtain a more complete understanding of the
90 cellularity of bacteria associated with mosquitoes, we assessed the invasive capability
91 of two common *Enterobacteriaceae* bacteria in mosquito cells using the gentamicin

invasion assay. Using this *in vitro* assay, we characterized the invasive process, examined the mechanisms by which bacteria invade cells, and assessed the effect of intracellular bacteria on host immunity and Zika virus (ZIKV) infection. Importantly, using mono-axenically infected mosquitoes, we found that these bacteria have intracellular localization in mosquitoes. This work expands our understanding of host-microbe interactions of gut-associated symbionts in medically relevant mosquito vectors at the cellular level.

Results and Discussion

Symbiotic bacteria invade mosquito cells *in vitro*

Horizontally acquired bacteria are generally considered to infect the gut lumen, they are also found in other organs of mosquitoes including the salivary glands, malpighian tubules, and germline [3, 4, 6, 25, 34]. It remains unknown how these tissues become infected, but it has been proposed these organs may act as a reservoir to facilitate transstadial transmission of microbes between mosquito life stages [4, 5]. One possibility is that gut bacteria exploit their intracellular lifestyle to transition between host tissues. Therefore, we investigated the capacity of bacteria commonly found in the gut of mosquitoes to invade mosquito host cells. We isolated two bacteria within the *Enterobacteriaceae* family, *Serratia marcescens* and *Cedecea neteri,* by conventional microbiological culturing approaches, and evaluated their invasive capacity using the gentamicin invasion assay [35].

While invasion assays are routinely used for pathogenic bacteria in mammalian cells, the assay is not commonly undertaken with mosquito cells. We performed the gentamicin invasion assay in Aag2 (*Aedes aegypti*) and Sua5B (*Anopheles gambiae*) cell lines comparing the invasion of *E. coli* BL21 (DE3) with or without the *Yersinia pseudotuberculosis* (*Yp*) *invasin* (*inv*) gene to invasion of these bacteria in Vero cells (Monkey Kidney cells). In mammalian systems, heterologous expression of the *Ypinv* gene facilitates invasion of *E. coli* into cell lines [36-38]. Similar to mammalian systems, we found that *E. coli* expressing the *Ypinv* gene had significantly increased invasion in Aag2 cells compared to the non-invasive *E. coli* control (Fig. S1, Unpaired t test, $p < 0.05$), while no statistical difference was seen in the Sua5B cell line, likely due to high variability among replicates ($p > 0.05$, Unpaired t test). As expected, *E. coli* expressing the *inv* gene invaded at significantly higher rates in Vero cells compared to non-invasive *E. coli* ($p < 0.05$, Unpaired t test). While several insect cell lines are naturally phagocytic [39, 40], our data suggested bacteria were actively invading Aag2 cells, and as such, we conducted the majority of our experiments with this cell line. Next, we completed the gentamicin invasion assay with the two gut-associated bacteria from mosquitoes, *C. neteri* and *S. marcescens,* and used *E. coli* with and without the *Ypinv* gene as the positive and negative controls, respectively. The native symbionts exhibited significantly higher rates of invasion compared to the *E. coli* expressing *Ypinv* (ANOVA with Tukey's multiple comparision test, $p < 0.05$) or wildtype *E. coli* (Fig. 1A, ANOVA with Tukey's multiple comparision test, $p < 0.01$) indicating native gut-associated microbes have the capacity to invade insect cells and are more adept at this process compared to non-native *E. coli* expressing mammalian invasive factors.

To further confirm the results from the gentamicin invasion assay, fluorescent and transmission electron microscopy (TEM) were performed on cells after invasion. In order to observe the invaded bacteria in cells using fluorescent microscopy, bacteria were transformed with a plasmid that expressed the mCherry fluorescent protein [41]. Similar to our quantitative results from the invasion assay, we observed a greater number of intracellular bacteria in the *Serratia* and *Cedecea* treatments compared to the *E. coli* negative control (Fig. 1B and Fig. S2). TEM images confirmed both symbionts isolated from mosquitoes were intracellular, and that bacteria were inside a vacuole (Fig. 1B, black arrowhead). *E. coli* did not invade cells and was found exclusively extracellularly. Bacterial encapsulation within a vacuole is a typical signature of invading bacteria in mammalian systems [42] as well as obligatory intracellular bacteria of insects such as *Wolbachia* [43]. Taken together, it is evident that both symbionts isolated from the mosquitoes can invade the host cells *in vitro*.

Next, we characterized the invasion process of *Cedecea* examining how the multiplicity of infection (MOI) and incubation time influenced invasion. We noted a linear increase in the number of intracellular *Cedecea* with increasing multiplicity of infection (MOI) (Fig. 1C, ANOVA with Tukey's multiple comparision test, $p < 0.05$). We then varied the invasion time and observed bacterial invasion as early as 15 minutes post infection and invasion increased until 8 hr post infection (Fig. 1D, ANOVA with Tukey's multiple comparision test, $p < 0.05$). We also examined the invasive ability of *C. neteri* in different mosquito cells lines. The invasion of this bacterium was similar in both *Ae.*

aegypti cell lines Aag2 and RML-12 (Fig. 1E, Tukey's multiple comparision test, $p < 0.05$); however, a greater number of intracellular bacteria were seen in the Sua5B cells.

In vitro intracellular replication and egression of *Cedecea neteri*

While undertaking TEM, we captured an image of intracellular replication of *C. neteri* within mosquito cells (Fig. 2A). Given that bacteria were seen to replicate in the intracellular environment, we attempted to culture these bacteria in Aag2 cells in a similar manner to *in vitro* propagation of other intracellular bacteria such as *Wolbachia* [44]. However, our culturing attempts were unsuccessful as the cell culture media became contaminated with the innoculated *C. neteri,* despite the extracellular bacteria, which had not invaded, being killed by gentamicin treatment. We hypothesized that intracellular *Cedecea* were egressing from the cells and replicating within the cell culture media.

We therefore undertook experiments to quantify bacterial egression from the cells. After allowing *C. neteri* to invade, Aag2 cells were incubated with or without gentamicin and intracellular and extracellular bacteria were quantified over time. Within the cell, bacterial numbers remained constant in the presence of gentamicin while in the absence of antibiotic, there was an an approximate 10-fold increase at eight hours post infection (Fig. 2B, Unpaired t test, $p<0.05$). In the cell culture media, we observed a precipitous increase in bacteria in the absence of antibiotic and recovered little to no viable bacteria when antibiotics were included in the media (Fig. 2C, Unpaired t test, $p<0.05$). These data indicated that *C. neteri* was egressing from the cells, replicating in

the cell culture media in the absence of antibiotic and then re-invading mosquito cells, which accounted for the significantly higher titer of intracellular *Cedecea* in the non-antibiotic treated cells at 8 hours post infection. We found few changes in the total number of mosquito cells in gentamicin treated or untreated cells, although there was a subtle but significant reduction in cell number after 8 hours in the treatment without antibiotics (Fig. S3, Unpaired t test, $p<0.0001$). However, overall, these data indicated that bacterial invasion and egression were not overly detrimental to the host cells.

Host actin and integrin are important for *Cedecea neteri* invasion

The lack of damage to host cells indicates non-lysis mediated exit of bacteria from host cells. While this would be expected from a mutualistic or commensal gut-associated bacterium, even some pathogens such as *Mycobacteria*, *Shigella*, and *Chlamydia* use protrusions and non-lytic exocytosis to exit the host cells without lysis of host cells [45-48]. The former method involves membrane extensions containing bacteria mediated by actin polymerization and ultimately these protruded structures are engulfed by neighboring cells resulting in the transfer of content to adjoining cell [49]. We therefore hypothesized that *C. neteri* may use actin-based motility as a mechanism to invade and exit cells.

To determine the role of the actin cytoskeleton in invasion of bacteria into mosquito cells, we inhibited the polymerization of actin filaments using cytochalasin D [50]. We observed a 3-fold reduction in invasion of *Cedecea* in the presence of cytochalasin D (Fig. 3A, ANOVA with Tukey's multiple comparision test, $p< 0.001$). In contrast, there

206 was no change in intracellular bacteria when cells were treated with SP600125, which
207 inhibits phagocytosis in mosquito cells [51]. These data suggested that the actin
208 cytoskeleton is co-opted by *C. neteri* to gain access to the intracellular milieu, and that
209 phagocytosis played a minimal role in the invasion of bacteria. Similar processes have
210 been observed in other bacteria-host systems. For example, obligatory intracellular
211 bacteria such as *Rickettsia*, *Chlamydia*, and *Ehrlichia* hijack the host cell cytoskeletal
212 and surface proteins to invade, survive and spread within cells [52-54]
213
214 We then examined whether host receptors facilitate the bacterial entry into mosquito
215 cells. In mosquitoes, integrins are involved in the engulfment of *E. coli* and malaria
216 parasites [55], while pathogenic bacteria of humans also exploit these receptors to
217 invade mammalian host cells [56-58]. Using RNAi, we silenced the alpha and beta
218 subunit of the integrin receptor and challenged cells with *C. neteri*. After confirming
219 gene silencing (Fig. S4 A and B), we found significantly fewer intracellular bacteria after
220 knocking down the beta-integrin (Fig. 3B, ANOVA with Tukey's multiple comparision
221 test, $p < 0.05$), but no differences in the rate of *Cedecea* invasion when the alpha-
222 integrin gene was silenced (Fig. 3C, ANOVA with Tukey's multiple comparision test, $p >$
223 0.05). These results indicated that symbiotic *C. neteri* utilized actin filaments and the
224 beta-integrin receptor to gain entry into the host cells.
225
226 **Intracellular *Cedecea* reduces ZIKV replication in mosquito cells**
227 Midgut-associated bacteria can affect pathogens transmitted by mosquitoes by direct or
228 indirect interactions [59-61]. Therefore, we examined how intracellular *C. neteri* affected

229 viral infection. The symbiont significantly reduced ZIKV loads in cell lines compared to
230 uninfected controls at both two (Fig. 4A, Unpaired t test, $p < 0.05$) and four (Fig. 4B,
231 Unpaired t test, $p < 0.01$) days post virus infection (dpvi) (Fig 4A and 4B). Similar to
232 *Cedecea*, intracellular *Serratia* also significantly reduced ZIKV density by four logs
233 compared to the uninfected cells at four dpvi (Fig. 4C, ANOVA with Tukey's multiple
234 comparison test, $p < 0.05$). To determine how the density of bacteria influenced viral
235 infection, we infected cells at increasing bacterial MOIs before inoculating with virus. At
236 lower MOIs (1:1 and 1:2), *Cedecea* significantly reduced ZIKV compared to the *E. coli*
237 (MOI 1:1, Unpaired t test, $p <0.01$, MOI 1:2, Unpaired t test, $p <0.0001$). However, at
238 higher MOIs, we noted that both *Cedecea* and *E. coli* reduced ZIKV compared to the
239 uninfected control. The complete blockage of ZIKV at the higher MOIs suggested that
240 even non-invasive bacteria can overwhelm viral infection, likely by induction of the
241 immune effector molecules that are antagonistic to viral infection. Taken together, our
242 results suggested that members of *Enterobacteriaceae* that commonly infect
243 mosquitoes have the capacity to interfere with viral pathogens when they are
244 intracellular.
245
246 **_Cedecea_ invasion stimulates mosquito immunity**
247 There is a complex interplay between the host innate immune system and microbiota
248 which maintains microbiome homeostasis [16, 62, 63]. However, invading arboviral
249 pathogens are also susceptible to these immune pathways [64, 65] thereby providing an
250 indirect mechanism by which microbiota can interfere with pathogens. We therefore
251 examined the immune response of mosquito cells challenged with *Cedecea* or *E. coli*

252 comparing these responses to uninfected cells. We quantified the transcription factors
253 (*rRel1*, *rRel2* and *Stat*) and negative regulators (*Cactus*, *Caspar*, and *PIAS*) of the Toll,
254 IMD and Jak/Stat immune pathways as well as downstream effector molecules
255 (*gambicin*, *definsin* and *cecropin*). We found the NF-κB transcription factor *Rel2* was
256 significantly upregulated by *Cedecea* compared to both the *E. coli* (ANOVA with Tukey's
257 multiple comparison test, $p < 0.05$) and the uninfected control (ANOVA with Tukey's
258 multiple comparison test, $p < 0.01$), while a significant difference was only observed for
259 *Rel1* when the *Cedecea* treatment was compared to the uninfected control (ANOVA
260 with Tukey's multiple comparison test, $p < 0.05$; Fig 5A). The negative regulator of the
261 Toll pathway, *Cactus*, was significantly upregulated compared to both the *E. coli* (Fig.
262 5B, ANOVA with Tukey's multiple comparison test, $P < 0.05$) and uninfected control
263 (ANOVA with Tukey's multiple comparison test, $p < 0.01$), while no changes were seen
264 for *Caspar*, the negative regulator of the IMD pathway (Fig. 5B, ANOVA with Tukey's
265 multiple comparison test, $p>0.05$,). Similarly, no significant changes were observed for
266 genes in the Jak/Stat pathway. Taken together, these data suggested that the Toll and
267 IMD pathways were induced by invasion of *Cedecea* into mosquito cells. This is
268 consistent with previous observations which demonstrated interplay between native
269 microbiota and mosquito innate immune pathways [61, 66-68]. We observed dramatic
270 modulation of effector molecules with *Defensin*, *Cecropin* and *Gambicin,* all significantly
271 enhanced by *Cedecea*. Strikingly, *Cecropin* and *Defensin* expression was nearly 1000-
272 fold higher (Fig. 5C, Tukey's multiple comparison test, $p < 0.0001$) whereas *Gambicin*
273 (Fig. 5C, Tukey's multiple comparison test, $p <0.001$) was elevated 100-fold in cells
274 inoculated with *Cedecea* compared to the non-infected control. In mosquitoes, these

downstream effector molecules are co-regulated by the Toll and IMD pathways [66], which could explain their prolific enhancement given that intracellular *Cedecea* stimulated both pathways. As arboviral pathogens also interact with innate immune pathways, we examined gene expression in cells when co-infected with ZIKV and *C. neteri* focusing on the NF-κB transcription factors and negative regulators of the Toll and IMD pathways. Patterns of gene expression were similar to the ZIKV uninfected cells with the exception of *Cactus*, where no significant differences were seen across bacterial treatments (Fig. 5D and E), suggesting that ZIKV was stimulating the Toll pathway as the negative regulator was depleted when comparing to ZIKV uninfected cells.

Intracellular *Enterobacteriaceae* within the *Aedes* gut epithelium

To determine the capacity of *C. neteri* and *S. marcescens* to invade host cells *in vivo,* we reared *Ae. aegypti* mosquitoes mono-axenically with either symbiont and analyzed tissues from larvae and adults by TEM and Confocal Laser Scanning Microscopy (CLSM). While it was evident there was an accumulation of extracellular *Serratia* in the lumen of the larval gut (Fig. 6A-B), we also identified bacteria that were associated with the microvilli. Specifically, we found examples of *Serratia* in the process of transitioning to or from the midgut epithelial cells. We appreciate our results cannot conclusively determine if *Serratia* was in the process of invading or egressing from cells, but regardless, it suggested that the bacterium had been or was soon to be intracellular. Analysis of gut tissue isolated from adult *Ae. aegypti* mosquitoes infected with *C. neteri* revealed the presence of bacteria in the cytosol of epithelial cells (Fig. 6B). Closer

298 inspection of these images revealed the bacterium was localized within a vacuole (Fig.
299 6B, yellow insert), which is a typical signature of intracellular bacteria. Here, *C. neteri*
300 may be exiting the membrane (Fig. 6B, inserts, white arrow), suggesting these bacteria
301 can egress from the membrane bound compartment which could facilitate their
302 replication and spreading.–Egression and re-entry mechanisms are used by several
303 pathogenic bacteria like *Listeria monocytogenes* and *Shigella flexneri* to escape the
304 vacuoles to replicative niches [69]. We also confirmed the intracellular localization of *C.*
305 *neteri* in adult infected guts by CLSM. The orthogonal views of the 3D-reconstructed
306 tissues locate bacteria on the cells as well as inside cells of the posterior gut,
307 demonstrated by the co-localization of actin staining with mCherry signal from bacteria
308 (Fig. 6C, Fig. S5, Supplementary video 1). We also found bacteria inside the cells of the
309 Malpighian tubules (Fig. 6C, Fig. S5, Supplementary video 2). Altogether, TEM and
310 CLSM results clearly show bacteria residing inside the host cells *in vivo*.
311
312 Our data show that *Enterobacteriaceae* that commonly infect the gut of mosquitoes
313 have the capacity to invade mosquito cells *in vitro* and *in vivo*. To gain access and
314 persist in these cells, bacteria need to overcome the host immune response and the
315 peritrophic matrix (PM). The PM, which acts as a physical barrier that separates
316 epithelial cells from the gut lumen, is expressed constitutively in larvae and after a blood
317 meal in adults. In a range of arthropods, genes associated with the PM are induced by
318 bacteria [70] and in turn, the PM plays a pivotal role maintaining gut microbiome
319 homeostasis, either by protecting bacteria from the innate immune response or
320 restoring bacterial composition and adundance post blood meal [71]. While another

study has identified bacteria associating with the epithelium in *Anopheles* mosquitoes [72] our finding of intracellular bacteria residing within the midgut epithelium of larvae and adults indicates the PM is not completely effective at inhibiting microbiota or that bacteria invade these cells before the PM has established. Alternatively, bacteria may produce enzymes that degrade the PM in a similar fashion to malaria parasites that express chitenases [73].

In *Drosophila*, ingested *Serratia* (Db11) invaded the midgut epithlieum in flies with an impaired IMD pathway, but not wild type flies. However, this infection reduces survival [30]. Similarly, fungal infection of *Anopheles* mosquitoes enables gut bacteria to translocate to the hemolymph leading to systemic infection [29]. Similar to the observations in *Drosophila* [30], we saw intracellular bacteria infrequently in the mosquito gut, suggesting there were intrinsic factors limiting the systemic infection. Innate immunity may be respsonsible for maintaining homeostatsis, which would be consistent with our gene expression data, or alternatively, these mutualistic bacteria may exploit similar molecular processes as their pathogenic counterparts to overcome host immune pathways [74]. The intracellular lifestyle of bacteria and their ability to egress from cells likely facilitates microbial persistence in these holometabolous insects. Our finding of intracellular bacteria in the malpighian tubules further supports this theory as bacteria residing within this tissue are known to be transstadially transmitted [4].

Conclusions

343 In conclusion, we have shown through various *in vitro* and *in vivo* data that symbiotic
344 *Enterobacteriaceae* can invade and replicate intracellularly in mosquito cells. Bacterial
345 invasion is mediated by host actin filaments and beta-integrin receptors. Intracellular
346 bacteria dramatically upregulate host IMD and Toll immune pathways and substantially
347 reduce ZIKV density in cells. These data enhance our understanding of host-microbe
348 interactions in mosquitoes and point to a possible mechanism by which bacteria, which
349 are commonly associated with the midgut, could infect other tissues within mosquitoes.
350
351 **Material and Methods.**
352 **Ethics statement:** ZIKV, which was originally isolated from an *Ae. aegypti* mosquito
353 (Chiapas State, Mexico), was obtained from the World Reference Center for Emerging
354 Viruses and Arboviruses at the University of Texas Medical Branch (Galveston, TX).
355 Experimental work with the virus was approved by the University of Texas Medical
356 Branch Institutional Biosafety Committee (reference number 2016055).
357
358 **Isolation of bacteria from mosquitoes:** Lab reared *Ae. albopictus* mosquitoes were
359 collected and surface sterilized before homogenized in 500 µl of 1X PBS. Serial dilution
360 of homogenates was plated on LB agar plate to obtain isolated colonies. The single
361 colonies were picked, grown in LB medium before isolating genomic DNA. The 16S
362 rDNA PCR was performed as described previously [75] and the PCR product was
363 Sanger sequenced to identify the bacterial species. To further classify the gut-
364 associated bacteria we completed multilocus sequence typing (MLST) as described

365 previously [11, 76]. The MLST sequences were aligned, concatenated and maximum
366 likelihood tree was constructed using Seaview [77] (Fig. S6).
367
368 **Bacterial growth and cell culture:** Two bacterial isolates were grown in LB medium at
369 37°C. The overnight culture was appropriately diluted in Schneider's media (Gibco) to
370 obtain the MOI of 10 before the infection. The mosquito cell lines were maintained in
371 their respective medium at 28 °C. The *Ae. aegypti* cell line Aag2 [78] and Sua5B cells
372 were maintained in *Drosophila* Schneider's medium (Gibco) supplemented with 20%
373 FBS (Denville Scientific) and 1% penicillin/streptomycin (P/S; 100 Units/mL and 100
374 µg/mL respectively), RML-12 cells were maintained in Leibovitz' (L15) medium (Gibco)
375 containing 20% FBS and 10% tryptose phosphate broth. Vero cells (CCL-81) were
376 purchased from the American Type Culture Collection (Bethesda, MD, USA) and
377 maintained in DMEM supplemented with 5% FBS and 1% P/S (100 Units/mL and 100
378 µg/mL respectively) at 37 °C with 5% CO_2.
379
380 **Gentamicin invasion assay:** The gentamicin invasion assay was performed as
381 described elsewhere with minor alterations [33]. Aag2 cells were seeded at the density
382 of $1x10^5$/well in 24-well plate 48h prior to infection. On the day of infection, cells were
383 washed in Schneider's media (Gibco) and infected with 500 µl of bacterial suspension.
384 After incubating for 1h at 28 °C, bacteria were removed, and cells were washed once
385 with Schneider's medium and incubated with 200 µg/ml gentamicin for additional 1h to
386 kill extracellular bacteria. The invaded bacteria were recovered after washing the cells

387 twice with Schneider's media and lysing them in 500 µl of 1X PBS containing 0.05%
388 Triton X-100.
389
390 **Fluorescence and Transmission electron microscopy:** In order to assess the
391 invasion of symbionts fluorescent microscopy and TEM was performed on the Aag2
392 cells after allowing bacteria to invade. The bacteria were transformed with mCherry
393 expressing plasmid pRAM18dRGA-mCherry, which is a modified version of
394 pRAM18dRGA[MCS] [41]. Aag2 cells were fixed with 1% PFA (Electron Microscopy
395 Sciences, Hartfield, PA) for 30 min and permeabilized in 1X PBS+0.01 % Triton X-100
396 (Fischer Scientific) for 20 min following staining with Atto 488 Phalloidin (Sigma) as per
397 manufacturers recommendations. The cell nuclei were stained with DAPI after washing
398 the slides in 1X PBS. The slides were stored in Prolong-Antifade (Invitrogen). The
399 samples were observed using the Revolve-FL epifluorescence microscope (ECHOLAB).
400 For TEM, insect cells were fixed in fixative (2.5% formaldehyde, 0.1% glutaraldehyde,
401 0.03% picric acid, 0.03% $CaCl_2$ and 0.05 M cacodylate buffer at pH 7.3) and post fixed
402 in 1% osmium tetroxide for 1 h, stained *en bloc* in 2% aqueous uranyl acetate at 60 °C
403 for 20 min, dehydrated in a graded series of ethanol concentrations, and embedded in
404 epoxy resin, Poly/Bed 812. Ultrathin sections were cut on a Leica EM UC7 (Leica
405 Microsystems, Buffalo Grove, IL), placed on Formvar-carbon copper 200 mesh grids,
406 stained with lead citrate and examined in a Philips (FEI) CM-100 electron microscope at
407 60 kV. To assess the *in vivo* invasion in mosquito larvae and adults, guts were
408 dissected after surface sterilization in 1X PBS and then the tissue was fixed in fixative
409 (2.5% glutaraldehyde and 2% paraformaldehyde buffered with 0.1 M sodium

cacodylate) for 2 hours and post fixed in 1% osmium tetroxide for 1 h at room temperature. Then samples were dehydrated in a graded series of ethanol concentrations, and embedded in epoxy resin, Epon 812. The sections were prepared as described above and imaged in a Tecnai Spirit (FEI) transmission electron microscope at 80 kV. For Confocal Laser Scanning Microscopy, tissue samples were fixed in 1% PFA in 1X PBS for 30 min, then permebalized with 0.01% Triton X-100 in 1X PBS for 20 min before staining with SiR-actin Kit (Spirochrome AG, Switzerland) for 1 hour and DAPI (Applied Biosystems) for 15 min. Then tissue samples were embedded in 1% low-melting agarose with SlowFade Diamond mounting solution (Molecular Probes). Samples were imaged and 3D-reconstructed (1.3 mm sections) using a Zeiss LSM-800 and were analysed in Zen 3.0 (Zeiss) and Fiji (ImageJ).

Intracellular replication of *Cedecea neteri*: To assess the replication of bacteria inside the host cells as well as in the medium, the Aag2 cells innoculated with *C. neteri* were incubated with or without gentamicin for 8h at 28 °C. Every two hours, the supernatant was collected and serial dilutions were plated on LB agar plate to enumerate the bacterial quantity in the medium. The cells were washed two times with Schneider's medium before plating on agar plate.

Host cytoskeleton and Janus Kinase in *Cedecea neteri* invasion: The gentamicin invasion assay was performed in the presence of actin and Janus kinase (JAK) inhibitors. The assay was performed by pre-incubating Aag2 cells in presence of 10 or 20 μg/ml of Cytochalasin D (Sigma) and 30 or 60 μg/ml of Sp600125 (Sigma) for 1 hr.

433 The gentamicin invasion assay was performed as described above with the addition of
434 each specific drug. A 60 μg/ml of DMSO treatment was used as a control.
435
436 **RNAi mediated integrin gene silencing in Aag2 cells:** In order to assess the role of
437 host integrin receptors in the invasion of *C. neteri*, the integrin alpha and beta receptors
438 were depleted using RNAi. dsRNA was designed for AAEL001829 and AAEL014660
439 using E-RNAi [79] and amplified using primers with flanking T7 promoter sequence
440 using *Ae. aegypti* cDNA as a template. dsRNA was synthesized using the T7
441 megascript kit (Ambion). The primers are listed in the Table S1. dsDNA against GFP
442 was used as control. Aag2 cells were transfected with 0.5 μg of each dsRNA using
443 Lipofectamine™ RNAiMAX (Life Technologies) 48hrs prior to bacterial infection and the
444 gentamicin invasion assay.
445
446 **RT-qPCR analysis:** Total RNA was isolated from Aag2 cells and reverse transcribed
447 using the amfiRivert cDNA synthesis Platinum master mix (GenDepot, Barker, TX, USA)
448 containing a mixture of oligo(dT)18 and random hexamers. Real-time quantification was
449 performed in a StepOnePlus instrument (Applied Biosystems, Foster City, CA) in a 10 μl
450 reaction mixture containing 10-20 ng cDNA template, 1X PowerUp SYBR green master
451 mix (Applied Biosystems), and 1 μM (each) primer. The analysis was performed using
452 the threshold cycle (ΔΔ CT) (Livak) method [80]. Four independent biological replicates
453 were conducted, and all PCRs were performed in duplicate. In order to assess the
454 expression of innate immune genes, the invasion assay was performed as described
455 earlier and post 24-hr invasion cells were harvested to isolate RNA, followed by cDNA

456 synthesis and RT-qPCR for specific genes. The ribosomal protein S7 gene [81] was
457 used for normalization of cDNA templates. Primer sequences are listed in Table S1.
458
459 ***In vitro* vector competence of ZIKV in Aag2 cells:** The assay was performed in order
460 to assess the how intracellular bacteria modulate ZIKV infection *in vitro*. After the
461 gentamicin invasion assay with *C. neteri* at an MOI of 1:1, 1:2, 1:5 and 1:10. After 24
462 hrs, the supernatant was removed, and cells were washed twice with 1x PBS before
463 infecting with ZIKV (Mex 1-7 strain) [82] at an MOI of 1:0.1. After 4 days, supernatant
464 was collected and ZIKV was quantified by focus forming assay [82]. The experiment
465 was repeated three times.
466 **Gnotobiotic rearing and *in vivo* invasion in mosquitoes:** *Ae. aegypti* gnotobiotic
467 larvae were generated as previously described [83]. To synchronize hatching, sterile
468 eggs were transferred to a conical flask and placed under a vacuum for 45 min. To
469 verify sterility, larval water was plated on non-selective LB agar plates. Twenty L1 larvae
470 were transferred to a T75 tissue culture flask and inoculated with transgenic symbionts
471 possessing the pRAM18dRGA-mCherry at $1x10^7$. Bacterial cultures were quantified with
472 a spectrophotometer (DeNovix DS-11, DeNovix) and validated by plating and
473 determining colony forming units. L1 larvae grown without bacteria were used as
474 contamination control, and these mosquitoes did not reach pupation [83]. To feed
475 mosquitoes, ground fish food pellets were sterilized by autoclaving and then mixed with
476 sterile water. 60 µl of fish food (1 µg/µl) was fed to larvae on alternative days.
477
478 **Acknowledgements.**

We would like to thank the UTMB insectary core for providing the lab mosquitoes. GLH is supported by NIH grants (R21AI138074, R21AI124452 and R21AI129507), the Wolfson Foundation and Royal Society (RSWF\R1\180013), the John S. Dunn Foundation Collaborative Research Award, and the Centers for Disease Control and Prevention (Cooperative Agreement Number U01CK000512). The paper contents are solely the responsibility of the authors and do not necessarily represent the official views of the Centers for Disease Control and Prevention or the Department of Health and Human Services. This work was also supported by a James W. McLaughlin postdoctoral fellowship at the University of Texas Medical Branch to SH and a NIH T32 fellowship (2T32AI007526) to MAS and Anti-VeC AV/PP0021//1 to AAS. Microscopy core facility at NYBC was supported by NYBC intramural fund. Confocal imaging facilities were funded by a Wellcome Trust Multi-User Equipment Grant (104936/Z/14/Z).

Author Contributions

SH and GLH designed the experiments. SH, DV, ACS, MAS, and VLP completed the experiments. SH, DV, VLP, AKC, and GLH undertook analysis. SH, AKC, AAS, and GLH wrote and edited the manuscript and all authors agreed to the final version. GLH acquired the funding and supervised the work.

Figure legends

Figure 1. Invasion of symbiotic bacteria into mosquito cells. The gentamicin invasion assay was used to examine the invasive capacity of symbiotic *Enterobacteriaceae* bacteria isolated from *Aedes* mosquitoes (A). Non-invasive *E. coli* was used as negative control. *E. coli* expressing the *Yersinia inv (Ypinv)* gene was used as a positive control. The assay was repeated twice. Flourscent and transmission electron microscopy was used to visual intracellular bacteria (B). Bacteria expressed mCherry fluorescent protein (red), actin filaments were stained with Phalloidin (green) and DNA with DAPI (blue). Arrowheads in the TEM images indicate vacuoles containing bacteria. Scale bar is 500 nm. Density (C) and time dependent (D) invasion of *C. neteri* in Aag2 cells. The density dependant invasion assay (C) was replicated twice. The time dependant invasion assay was done at host cell: bacterial density of 1:10 (N=4). *C. neteri* invasion in *Aedes aegypti (*Aag2 and RML-12) *and Anopheles gambiae* (Sua5B) (E). The assay was repeated twice. Letters indicate significant differences ($p < 0.05$) determined by a One-Way ANOVA with a Tukey's multiple comparison test.

Figure 2. Intracellular replication and egression of *C. neteri* in Aag2 cells. TEM of Aag2 cells containing invaded *C. neteri* replicating inside Aag2 cell (A). Arrow indicates the dividing bacterial cell. Bacterial titer in cells (B) or in the cell culture media (C) in the presence and absence of gentamicin. The significance between the gentamicin and non-treated samples at different time post invasion was analyzed by Unpaired t test. Five replicates were used at each time point.

Figure 3. The role of host cytoskeletal proteins and receptors in the *C. neteri* invasion. Invasion of *C. neteri* in the presence of inhibotors of actin polymerisation (Cyt D) and phagocytosis (SP600125 [Sp]) (A). DMSO was used as control to assess its cytotoxic effect on the cells. *C. neteri* invasion after silencing of the beta- (B) and alpha- (C) integrins. The expeirments were repeated twice. Letters indicate significant differences ($p < 0.05$) determined by a One-Way ANOVA with a Tukey's multiple comparison test.

Figure 4. Intracellular bacteria reduces ZIKV titer in *Ae. aegypti* cells. ZIKV infection at 2 (A) and 4 (B) days post invasion compared to an uninfected control. ZIKV infection in *C. neteri* or *S. marcescens* infected cells (C). The effect of bacterial density on ZIKV infection (D). *C. neteri* and *E. coli* were inoculated onto cells using the gentamicin invasion assay at increasing MOIs. For the *C. neteri* 1:2, 1:5, and 1:10 and *E. coli* 1:10 treatments, no ZIKV was recovered from cells. For A, B and D significance was determind using unpaired t-test, while for C, significance was calculated by one-way ANNOVA with Tukey's multiple comparison test.

Figure 5. Intracellular *C. neteri* upregulates mosquito Toll and IMD innate immune pathways. Gene expression analysis of the NF-κB transcriptional activators (A) and the negative regulators (B) of the Toll, IMD and JAK-STAT pathways as well as downstream effector molecules (C). Gene expression was measured 24 hr post *C. neteri* invasion in Aag2 cells. Gene expression of the NF-κB transcriptional activators (D) and the negative regulators (E) in cells co-infected with *C. neteri* or *S. marcescens*

546 and ZIKV. 24 hours post bacterial infection cells were infected with ZIKV. Samples were
547 collected 4 days post ZIKV infection for qPCR analysis. The experiment was repeated
548 twice. Letters indicate significant differences ($p < 0.05$) determined by a One-Way
549 ANOVA with a Tukey's multiple comparison test.
550
551 **Figure 6. Intracellular localization of *C. neteri* and *S. marcescens* in mosquito**
552 **tissues.** TEM micrographs of *S. marcescens* (Sm) accumulated in the gut lumen and
553 associated with the microvilli of the gut epithelium in mono-axenically infected *Ae.*
554 *aegypti* adults (A). Magnified image of bacteria attaching to microvilli (MV) (B), and
555 bacteria in the process of entering or exiting the gut epithelia (purple and green insert).
556 (B) Intracellular *C. neteri* (Cn) in the larval gut mono-axenically infected *Ae. aegypti*.
557 Mitochondria (M) and nucleus (N). Yellow and blue inserts show larger view of bacteria
558 from B. CLSM evidence of the intracellular localization of *C. neteri* in the adult mosquito
559 gut and Malpighian tubules (C). Bright field (left) and maximum intensity projection
560 (right) of tissues 3D-reconstructed from a series of Z-stacks merging mosquito actin
561 (white), mCherry-expressing *C. neteri* (yellow) and DAPI-stained DNA (magenta). Two
562 representative XZ and YZ orthogonal views (OV1-4) of the stacks are shown for each
563 tissue on the sides, and the identity of intracellular bacteria examples is noted with
564 colored squares. On the right, the plots coloured according to the identity of the
565 corresponding bacterium, show the co-localization of the actin signal (gray) with the
566 mCherry bacteria (yellow). Scale bars are 50 μm.
567
568

Supplementary figure legends

Figure S1. Gentamicin invasion assay in different cell lines. Invasion of *E. coli* and *E. coli BL21* expressing the *Yersina invasion* gene (*Ypinv*) in different cell lines. The assay was done in Aag2 (*Aedes aegypti*), Sua5B (*Anopheles gambiae*) and Vero (Monkey kidney cells). The assay was done twice. The statistical significance was determined using an Unpaired t-test.

Figure S2. Flourscent microscopy of bacteria in Aag2 cells. Merged and separate channels – blue (DAPI), green (actin filaments stained with Phalloidin), red (bacteria expressing mCherry). Scale bars are 70 μm.

Figure S3. Effect of intracellular bacteria on the cell viability. Aag2 cell numbers at different times post invasion with *C. neteri.* Cells were supplement with gentamicin (200 μg/ml) or cultured in the absence of antibiotic.

Figure S4. Validation of gene silencing in cells. RT-qPCR analysis of beta (A) and alpha (B) integrin gene expression 24 hours post transfection of dsRNA. dsRNAs targetting GFP were used as the negative control. The experiment was repeated twice. The statistical significance was determined using an Unpaired t-test.

Figure S5. CLSM analyses of infected adult gut and Malpighian tubule. Maximum intensity projection of tissues 3D-reconstructed from a series of Z-stacks merging mosquito actin (white), mCherry-expressing *Cedecea* (yellow) and DAPI-stained DNA

(magenta). Several XZ and YZ orthogonal views (OV) of the stacks are shown for each tissue on the sides. Scale bars are 50 μm.

Figure S6. Multilocus sequence analysis according to [76] indicates isolate to be members of the *S. marcescens* species; the MLST genes were amplified from bacteria isolated from *Aedes albopictus* mosquitoes (highlighted in blue).

Supplementary table legends.

Table S1. Primer sequences used in this study

Supplementary video legends.

Video S1. Series of Z-stacks of an adult infected gut by CLSM.

Video S2. Series of Z-stacks of an adult infected Malpighian tubule by CLSM.

607 **Reference:**

608

609 1. Duguma D, Hall MW, Smartt CT, Neufeld JD. Effects of Organic Amendments on
610 Microbiota Associated with the Culex nigripalpus Mosquito Vector of the Saint Louis
611 Encephalitis and West Nile Viruses. mSphere. 2017;2(1). Epub 2017/02/09. doi:
612 10.1128/mSphere.00387-16.
613 2. Dada N, Jumas-Bilak E, Manguin S, Seidu R, Stenström T-A, Overgaard HJ.
614 Comparative assessment of the bacterial communities associated with Aedes aegypti
615 larvae and water from domestic water storage containers. Parasites &
616 Vectors. 2014;7(1):391. doi: 10.1186/1756-3305-7-391.
617 3. Gusmao DS, Santos AV, Marini DC, Russo Ede S, Peixoto AM, Bacci Junior M,
618 et al. First isolation of microorganisms from the gut diverticulum of Aedes aegypti
619 (Diptera: Culicidae): new perspectives for an insect-bacteria association. Mem Inst
620 Oswaldo Cruz. 2007;102(8):919-24. Epub 2008/01/23. doi: 10.1590/s0074-
621 02762007000800005.
622 4. Chavshin AR, Oshaghi MA, Vatandoost H, Yakhchali B, Zarenejad F, Terenius
623 O. Malpighian tubules are important determinants of Pseudomonas transstadial
624 transmission and longtime persistence in Anopheles stephensi. Parasites &
625 Vectors. 2015;8(1):36. doi: 10.1186/s13071-015-0635-6.
626 5. Chen S, Bagdasarian M, Walker ED. *Elizabethkingia anophelis*: Molecular
627 Manipulation and Interactions with Mosquito Hosts. Applied and Environmental
628 Microbiology. 2015;81(6):2233. doi: 10.1128/AEM.03733-14.

6. Alonso DP, Mancini MV, Damiani C, Cappelli A, Ricci I, Alvarez MVN, et al. Genome Reduction in the Mosquito Symbiont Asaia. Genome Biol Evol. 2019;11(1):1-10. Epub 2018/11/27. doi: 10.1093/gbe/evy255.

7. Duguma D, Hall MW, Smartt CT, Debboun M, Neufeld JD. Microbiota variations in Culex nigripalpus disease vector mosquito of West Nile virus and Saint Louis Encephalitis from different geographic origins. PeerJ. 2019;6:e6168. Epub 2019/01/16. doi: 10.7717/peerj.6168.

8. Osei-Poku J, Mbogo CM, Palmer WJ, Jiggins FM. Deep sequencing reveals extensive variation in the gut microbiota of wild mosquitoes from Kenya. Molecular Ecology. 2012;21(20):5138-50. doi: 10.1111/j.1365-294X.2012.05759.x.

9. Muturi EJ, Ramirez JL, Rooney AP, Kim C-H. Comparative analysis of gut microbiota of mosquito communities in central Illinois. PLoS Neglected Tropical Diseases. 2017;11(2):e0005377-18. doi: 10.1371/journal.pntd.0005377.

10. Pei D, Jiang J, Yu W, Kukutla P, Uentillie A, Xu J. The *waaL* gene mutation compromised the inhabitation of *Enterobacter sp. Ag1* in the mosquito gut environment. Parasites & Vectors. 2015:1-10. doi: 10.1186/s13071-015-1049-1.

11. Hegde S, Nilyanimit P, Kozlova E, Anderson ER, Narra HP, Sahni SK, et al. CRISPR/Cas9-mediated gene deletion of the ompA gene in symbiotic Cedecea neteri impairs biofilm formation and reduces gut colonization of Aedes aegypti mosquitoes. PLOS Neglected Tropical Diseases. 2019;13(12):e0007883. doi: 10.1371/journal.pntd.0007883.

650 12. Guegan M, Zouache K, Demichel C, Minard G, Tran Van V, Potier P, et al. The
651 mosquito holobiont: fresh insight into mosquito-microbiota interactions. Microbiome.
652 2018;6(1):49. Epub 2018/03/21. doi: 10.1186/s40168-018-0435-2.
653 13. Brady OJ, Godfray HC, Tatem AJ, Gething PW, Cohen JM, McKenzie FE, et al.
654 Vectorial capacity and vector control: reconsidering sensitivity to parameters for malaria
655 elimination. Trans R Soc Trop Med Hyg. 2016;110(2):107-17. Epub 2016/01/30. doi:
656 10.1093/trstmh/trv113.
657 14. Hegde S, Rasgon JL, Hughes GL. The microbiome modulates arbovirus
658 transmissionin mosquitoes. Current Opinion in Virology. 2015;15:97-102. doi:
659 10.1016/j.coviro.2015.08.011.
660 15. Caragata EP, Tikhe CV, Dimopoulos G. Curious entanglements: interactions
661 between mosquitoes, their microbiota, and arboviruses. Current Opinion in Virology.
662 2019;37:26-36. doi: https://doi.org/10.1016/j.coviro.2019.05.005.
663 16. Saldaña MA, Hegde S, Hughes GL. Microbial control of arthropod-borne disease.
664 Memórias do Instituto Oswaldo Cruz. 2017;112(2):81-93. doi: 10.1590/0074-
665 02760160373.
666 17. Ricci I, Damiani C, Capone A, DeFreece C, Rossi P, Favia G.
667 Mosquito/microbiota interactions: from complex relationships to biotechnological
668 perspectives. Current Opinion in Microbiology. 2012;15(3):278-84. doi:
669 10.1016/j.mib.2012.03.004.
670 18. Berhanu A, Abera A, Nega D, Mekasha S, Fentaw S, Assefa A, et al. Isolation
671 and identification of microflora from the midgut and salivary glands of Anopheles

672 species in malaria endemic areas of Ethiopia. BMC Microbiol. 2019;19(1):85. Epub
673 2019/05/01. doi: 10.1186/s12866-019-1456-0.
674 19. Dickson LB, Ghozlane A, Volant S, Bouchier C, Ma L, Vega-Rua A, et al. Diverse
675 laboratory colonies of Aedes aegypti harbor the same adult midgut bacterial
676 microbiome. Parasites & Vectors. 2018;11(1):207. doi: 10.1186/s13071-018-
677 2780-1.
678 20. Damiani C, Ricci I, Crotti E, Rossi P, Rizzi A, Scuppa P, et al. Paternal
679 transmission of symbiotic bacteria in malaria vectors. Current biology : CB.
680 2008;18(23):R1087-8. doi: 10.1016/j.cub.2008.10.040.
681 21. Sharma P, Sharma S, Maurya RK, Das De T, Thomas T, Lata S, et al. Salivary
682 glands harbor more diverse microbial communities than gut in Anopheles culicifacies.
683 Parasites & Vectors. 2014;7(1):235. doi: 10.1186/1756-3305-7-235.
684 22. Gimonneau G, Tchioffo MT, Abate L, Boissière A, Awono-Ambene PH, Nsango
685 SE, et al. Composition of Anopheles coluzzii and Anopheles gambiae microbiota from
686 larval to adult stages. Infection, genetics and evolution : journal of molecular
687 epidemiology and evolutionary genetics in infectious diseases. 2014;28:715-24. doi:
688 10.1016/j.meegid.2014.09.029.
689 23. Mancini MV, Damiani C, Accoti A, Tallarita M, Nunzi E, Cappelli A, et al.
690 Estimating bacteria diversity in different organs of nine species of mosquito by next
691 generation sequencing. BMC Microbiol. 2018;18(1):126. Epub 2018/10/06. doi:
692 10.1186/s12866-018-1266-9.
693 24. Segata N, Baldini F, Pompon J, Garrett WS, Truong DT, Dabiré RK, et al. The
694 reproductive tracts of two malaria vectors are populated by a core microbiome and by

695 gender- and swarm-enriched microbial biomarkers. Scientific Reports. 2016;6:24207.
696 doi: 10.1038/srep24207.
697 25. Tchioffo MT, Boissiere A, Abate L, Nsango SE, Bayibeki AN, Awono-Ambene
698 PH, et al. Dynamics of Bacterial Community Composition in the Malaria Mosquito's
699 Epithelia. Front Microbiol. 2015;6:1500. Epub 2016/01/19. doi:
700 10.3389/fmicb.2015.01500.
701 26. Koosha M, Vatandoost H, Karimian F, Choubdar N, Oshaghi MA. Delivery of a
702 Genetically Marked Serratia AS1 to Medically Important Arthropods for Use in RNAi and
703 Paratransgenic Control Strategies. Microb Ecol. 2018. Epub 2018/11/22. doi:
704 10.1007/s00248-018-1289-7.
705 27. Wang S, Dos-Santos ALA, Huang W, Liu KC, Oshaghi MA, Wei G, et al. Driving
706 mosquito refractoriness to *Plasmodium falciparum* with engineered symbiotic bacteria.
707 Science (New York, NY). 2017;357(6358):1399-402. doi: 10.1126/science.aan5478.
708 28. Damiani C, Ricci I, Crotti E, Rossi P, Rizzi A, Scuppa P, et al. Mosquito-Bacteria
709 Symbiosis: The Case of Anopheles gambiae and Asaia. Microb Ecol. 2010;60(3):644-
710 54. doi: 10.1007/s00248-010-9704-8.
711 29. Wei G, Lai Y, Wang G, Chen H, Li F, Wang S. Insect pathogenic fungus interacts
712 with the gut microbiota to accelerate mosquito mortality. Proceedings of the National
713 Academy of Sciences of the United States of America. 2017;114(23):5994-9. doi:
714 10.1073/pnas.1703546114.
715 30. Nehme NT, Liégeois S, Kele B, Giammarinaro P, Pradel E, Hoffmann JA, et al. A
716 model of bacterial intestinal infections in Drosophila melanogaster. 2007;3(11):e173.
717 doi: 10.1371/journal.ppat.0030173.

718 31. Czuczman MA, Fattouh R, van Rijn JM, Canadien V, Osborne S, Muise AM, et
719 al. Listeria monocytogenes exploits efferocytosis to promote cell-to-cell spread. Nature.
720 2014;509(7499):230-4. Epub 2014/04/18. doi: 10.1038/nature13168.
721 32. Ribet D, Cossart P. How bacterial pathogens colonize their hosts and invade
722 deeper tissues. Microbes and infection. 2015;17(3):173-83. doi:
723 10.1016/j.micinf.2015.01.004.
724 33. Hegde S, Hegde S, Spergser J, Brunthaler R, Rosengarten R, Chopra-
725 Dewasthaly R. In vitro and in vivo cell invasion and systemic spreading of Mycoplasma
726 agalactiae in the sheep infection model. International journal of medical microbiology :
727 IJMM. 2014;304(8):1024-31. doi: 10.1016/j.ijmm.2014.07.011.
728 34. Tchioffo MT, Abate L, Boissière A, Nsango SE, Gimonneau G, Berry A, et al. An
729 epidemiologically successful Escherichia coli sequence type modulates Plasmodium
730 falciparum infection in the mosquito midgut. Infection, genetics and evolution : journal of
731 molecular epidemiology and evolutionary genetics in infectious diseases. 2016;43:22-
732 30. doi: 10.1016/j.meegid.2016.05.002.
733 35. Elsinghorst EA. Measurement of invasion by gentamicin resistance. Methods
734 Enzymol. 1994;236:405-20. Epub 1994/01/01.
735 36. Isberg RR, Falkow S. A single genetic locus encoded by Yersinia
736 pseudotuberculosis permits invasion of cultured animal cells by Escherichia coli K-12.
737 Nature. 1985;317(6034):262-4.
738 37. Isberg RR, Voorhis DL, Falkow S. Identification of invasin: a protein that allows
739 enteric bacteria to penetrate cultured mammalian cells. Cell. 1987;50(5):769-78. Epub
740 1987/08/28. doi: 10.1016/0092-8674(87)90335-7.

741 38. Dersch P, Isberg RR. A region of the Yersinia pseudotuberculosis invasin protein
742 enhances integrin-mediated uptake into mammalian cells and promotes self-
743 association. The EMBO Journal. 1999;18(5):1199-213. doi: 10.1093/emboj/18.5.1199.
744 39. Trujillo-Ocampo A, Cazares-Raga FE, Del Angel RM, Medina-Ramirez F,
745 Santos-Argumedo L, Rodriguez MH, et al. Participation of 14-3-3epsilon and 14-3-3zeta
746 proteins in the phagocytosis, component of cellular immune response, in Aedes
747 mosquito cell lines. Parasit Vectors. 2017;10(1):362. Epub 2017/08/03. doi:
748 10.1186/s13071-017-2267-5.
749 40. Dimopoulos G, Müller HM, Levashina EA, Kafatos FC. Innate immune defense
750 against malaria infection in the mosquito. Current Opinion in Immunology.
751 2001;13(1):79-88.
752 41. Hegde S, Khanipov K, Albayrak L, Golovko G, Pimenova M, Saldaña MA, et al.
753 Microbiome interaction networks and community structure from laboratory-reared and
754 field-collected *Aedes aegypti*, *Aedes albopictus*, and *Culex quinquefasciatus* mosquito
755 vectors. Frontiers in Microbiology. 2018;9:715. doi: 10.3389/fmicb.2018.02160.
756 42. Gupta L, Molina-Cruz A, Kumar S, Rodrigues J, Dixit R, Zamora RE, et al. The
757 STAT pathway mediates late-phase immunity against Plasmodium in the mosquito
758 Anopheles gambiae. Cell Host & Microbe. 2009;5(5):498-507. doi:
759 10.1016/j.chom.2009.04.003.
760 43. Wright JD, Barr AR. The ultrastructure and symbiotic relationships of Wolbachia
761 of mosquitoes of the Aedes scutellaris group. Journal of Ultrastructure Research.
762 1980;72(1):52-64. doi: https://doi.org/10.1016/S0022-5320(80)90135-5.

763 44. Fattouh N, Cazevieille C, Landmann F. Wolbachia endosymbionts subvert the
764 endoplasmic reticulum to acquire host membranes without triggering ER stress. PLOS
765 Neglected Tropical Diseases. 2019;13(3):e0007218. doi: 10.1371/journal.pntd.0007218.
766 45. Traven A, Naderer T. Microbial egress: a hitchhiker guide to freedom. PLOS
767 Pathogens. 2014;10(7):e1004201. doi: 10.1371/journal.ppat.1004201.
768 46. Flieger A, Frischknecht F, Hacker G, Hornef MW, Pradel G. Pathways of host cell
769 exit by intracellular pathogens. Microb Cell. 2018;5(12):525-44. Epub 2018/12/12. doi:
770 10.15698/mic2018.12.659.
771 47. Haglund CM, Welch MD. Pathogens and polymers: microbe-host interactions
772 illuminate the cytoskeleton. J Cell Biol. 2011;195(1):7-17. Epub 2011/10/05. doi:
773 10.1083/jcb.201103148.
774 48. Hybiske K, Stephens R. Cellular Exit Strategies of Intracellular Bacteria.
775 Microbiol Spectr. 2015;3(6). Epub 2016/06/24. doi: 10.1128/microbiolspec.VMBF-0002-
776 2014.
777 49. Fukumatsu M, Ogawa M, Arakawa S, Suzuki M, Nakayama K, Shimizu S, et al.
778 Shigella targets epithelial tricellular junctions and uses a noncanonical clathrin-
779 dependent endocytic pathway to spread between cells. Cell Host & Microbe.
780 2012;11(4):325-36. doi: 10.1016/j.chom.2012.03.001.
781 50. Casella JF, Flanagan MD, Lin S. Cytochalasin D inhibits actin polymerization and
782 induces depolymerization of actin filaments formed during platelet shape change.
783 Nature. 1981;293(5830):302-5. Epub 1981/09/24. doi: 10.1038/293302a0.
784 51. Mizutani T, Kobayashi M, Eshita Y, Shirato K, Kimura T, Ako Y, et al.
785 Involvement of the JNK-like protein of the Aedes albopictus mosquito cell line, C6/36, in

786 phagocytosis, endocytosis and infection of West Nile virus. Insect Mol Biol. 2003;12.
787 doi: 10.1046/j.1365-2583.2003.00435.x.
788 52. Lin M, Kikuchi T, Brewer HM, Norbeck AD, Rikihisa Y. Global Proteomic Analysis
789 of Two Tick-Borne Emerging Zoonotic Agents: Anaplasma Phagocytophilum and
790 Ehrlichia Chaffeensis. Frontiers in Microbiology. 2011;2. doi:
791 10.3389/fmicb.2011.00024.
792 53. Martinez JJ, Cossart P. Early signaling events involved in the entry of Rickettsia
793 conorii into mammalian cells. Journal Of Cell Science. 2004;117(Pt 21):5097-106. doi:
794 10.1242/jcs.01382.
795 54. Wesolowski J, Paumet F. Taking control: reorganization of the host cytoskeleton
796 byChlamydia. F1000Research. 2017;6:2058. doi: 10.12688/f1000research.12316.1.
797 55. Moita L, Vriend G, Mahairaki V, Louis C, Kafatos F. Integrins of Anopheles
798 gambiae and a putative role of a new β integrin, BINT2, in phagocytosis of E. coli. Insect
799 Biochemistry and Molecular Biology. 2006;36(4):282-90. doi:
800 10.1016/j.ibmb.2006.01.004.
801 56. Eto DS, Jones TA, Sundsbak JL, Mulvey MA. Integrin-mediated host cell
802 invasion by type 1-piliated uropathogenic Escherichia coli. PLOS Pathogens.
803 2007;3(7):e100. doi: 10.1371/journal.ppat.0030100.
804 57. Wu J, Weening EH, Faske JB, Höök M, Skare JT. Invasion of Eukaryotic Cells by
805 Borrelia burgdorferiRequires β 1Integrins and Src Kinase Activity. Infection and
806 Immunity. 2011;79(3):1338-48. doi: 10.1128/IAI.01188-10.

807 58. Gillenius E, Urban CF. The adhesive protein invasin of Yersinia
808 pseudotuberculosis induces neutrophil extracellular traps via β1 integrins. Microbes and
809 infection. 2015;17(5):327-36. doi: 10.1016/j.micinf.2014.12.014.
810 59. Miesen P, van Rij RP. Crossing the Mucosal Barrier: A Commensal Bacterium
811 Gives Dengue Virus a Leg-Up in the Mosquito Midgut. Cell Host Microbe. 2019;25(1):1-
812 2. Epub 2019/01/11. doi: 10.1016/j.chom.2018.12.009.
813 60. Coatsworth H, Caicedo PA, Van Rossum T, Ocampo CB, Lowenberger C. The
814 Composition of Midgut Bacteria in Aedes aegypti (Diptera: Culicidae) That Are Naturally
815 Susceptible or Refractory to Dengue Viruses. Journal of Insect Science. 2018;18(6).
816 doi: 10.1093/jisesa/iey118.
817 61. Hegde S, Hegde S, Hegde S, Zimmermann M, Flöck M, Spergser J, et al.
818 Simultaneous Identification of Potential Pathogenicity Factors of Mycoplasma agalactiae
819 in the Natural Ovine Host by Negative Selection. Infection and Immunity.
820 2015;83(7):2751-61. doi: 10.1128/IAI.00403-15.
821 62. Broderick NA. Friend, foe or food? Recognition and the role of antimicrobial
822 peptides in gut immunity and Drosophila-microbe interactions. Philosophical
823 transactions of the Royal Society of London Series B, Biological sciences.
824 2016;371(1695):20150295. doi: 10.1098/rstb.2015.0295.
825 63. Buchon N, Broderick NA, Poidevin M, Pradervand S, Lemaitre B. Drosophila
826 intestinal response to bacterial infection: activation of host defense and stem cell
827 proliferation. Cell Host & Microbe. 2009;5(2):200-11. doi:
828 10.1016/j.chom.2009.01.003.

829 64. Cheng G, Liu Y, Wang P, Xiao X. Mosquito Defense Strategies against Viral
830 Infection. Trends Parasitol. 2016;32(3):177-86. Epub 2015/12/03. doi:
831 10.1016/j.pt.2015.09.009.
832 65. Fragkoudis R, Attarzadeh-Yazdi G, Nash AA, Fazakerley JK, Kohl A. Advances
833 in dissecting mosquito innate immune responses to arbovirus infection. The Journal of
834 general virology. 2009;90(Pt 9):2061-72. doi: 10.1099/vir.0.013201-0.
835 66. Zhang X, Aksoy E, Girke T, Raikhel AS, Karginov FV. Transcriptome-wide
836 microRNA and target dynamics in the fat body during the gonadotrophic cycle of Aedes
837 aegypti. Proceedings of the National Academy of Sciences of the United States of
838 America. 2017;114(10):E1895-E903. doi: 10.1073/pnas.1701474114.
839 67. Barletta AB, Nascimento-Silva MC, Talyuli OA, Oliveira JH, Pereira LO, Oliveira
840 PL, et al. Microbiota activates IMD pathway and limits Sindbis infection in Aedes
841 aegypti. Parasit Vectors. 2017;10(1):103. Epub 2017/02/25. doi: 10.1186/s13071-017-
842 2040-9.
843 68. Kumar A, Srivastava P, Sirisena P, Dubey SK, Kumar R, Shrinet J, et al.
844 Mosquito Innate Immunity. Insects. 2018;9(3). Epub 2018/08/12. doi:
845 10.3390/insects9030095.
846 69. Friedrich N, Hagedorn M, Soldati-Favre D, Soldati T. Prison break: pathogens
847 strategies to egress from host cells. Microbiol Mol Biol Rev. 2012;76(4):707-20. doi:
848 10.1128/MMBR.00024-12.
849 70. Narasimhan S, Rajeevan N, Liu L, Zhao YO, Heisig J, Pan J, et al. Gut
850 Microbiota of the Tick Vector Ixodes scapularis Modulate Colonization of the Lyme

851 Disease Spirochete. Cell Host & Microbe. 2014;15(1):58-71. doi:
852 10.1016/j.chom.2013.12.001.
853 71. Rodgers FH, Gendrin M, Wyer CAS, Christophides GK. Microbiota-induced
854 peritrophic matrix regulates midgut homeostasis and prevents systemic infection of
855 malaria vector mosquitoes. PLOS Pathogens. 2017;13(5):e1006391. doi:
856 10.1371/journal.ppat.1006391.
857 72. Gusmão DS, Santos AV, Marini DC, Bacci Jr M, Berbert-Molina MA, Lemos FJA.
858 Culture-dependent and culture-independent characterization of microorganisms
859 associated with Aedes aegypti (Diptera: Culicidae) (L.) and dynamics of bacterial
860 colonization in the midgut. Acta Tropica. 2010;115(3):275-81. doi:
861 10.1016/j.actatropica.2010.04.011.
862 73. Tsai YL, Hayward RE, Langer RC, Fidock DA, Vinetz JM. Disruption of
863 Plasmodium falciparum Chitinase Markedly Impairs Parasite Invasion of Mosquito
864 Midgut. Infection and Immunity. 2001;69(6):4048-54. doi: 10.1128/IAI.69.6.4048-
865 4054.2001.
866 74. Goebel W, Gross R. Intracellular survival strategies of mutualistic and parasitic
867 prokaryotes. Trends Microbiol. 2001;9(6):267-73. Epub 2001/06/08.
868 75. Kumar S, Molina-Cruz A, Gupta L, Rodrigues J, Barillas-Mury C. A
869 peroxidase/dual oxidase system modulates midgut epithelial immunity in *Anopheles*
870 *gambiae*. Science. 2010;327(5973):1644-8. doi: 10.1126/science.1184008.
871 76. Brady C, Cleenwerck I, Venter S, Coutinho T, De Vos P. Taxonomic evaluation
872 of the genus Enterobacter based on multilocus sequence analysis (MLSA): Proposal to
873 reclassify E. nimipressuralis and E. amnigenus into Lelliottia gen. nov. as Lelliottia

874 nimipressuralis comb. nov. and Lelliottia amnigena comb. nov., respectively, E.
875 gergoviae and E. pyrinus into Pluralibacter gen. nov. as Pluralibacter gergoviae comb.
876 nov. and Pluralibacter pyrinus comb. nov., respectively, E. cowanii, E. radicincitans, E.
877 oryzae and E. arachidis into Kosakonia gen. nov. as Kosakonia cowanii comb. nov.,
878 Kosakonia radicincitans comb. nov., Kosakonia oryzae comb. nov. and Kosakonia
879 arachidis comb. nov., respectively, and E. turicensis, E. helveticus and E. pulveris into
880 Cronobacter as Cronobacter zurichensis nom. nov., Cronobacter helveticus comb. nov.
881 and Cronobacter pulveris comb. nov., respectively, and emended description of the
882 genera Enterobacter and Cronobacter. Systematic and Applied Microbiology.
883 2013;36(5):309-19. doi: https://doi.org/10.1016/j.syapm.2013.03.005.
884 77. Gouy M, Guindon S, Gascuel O. SeaView version 4: A multiplatform graphical
885 user interface for sequence alignment and phylogenetic tree building. Molecular biology
886 and evolution. 2010;27(2):221-4. Epub 2009/10/23. doi: 10.1093/molbev/msp259.
887 78. Peleg J. Growth of arboviruses in primary tissue culture of Aedes aegypti
888 embryos. Am J Trop Med Hyg. 1968;17.
889 79. Horn T, Boutros M. E-RNAi: a web application for the multi-species design of
890 RNAi reagents--2010 update. Nucleic Acids Research. 2010;38(Web Server
891 issue):W332-9. doi: 10.1093/nar/gkq317.
892 80. Livak KJ, Schmittgen TD. Analysis of Relative Gene Expression Data Using
893 Real-Time Quantitative PCR and the 2−ΔΔCT Method. Methods (San Diego, Calif).
894 2001;25(4):402-8. doi: 10.1006/meth.2001.1262.
895 81. Isoe J, Collins J, Badgandi H, Day WA, Miesfeld RL. Defects in coatomer protein
896 I (COPI) transport cause blood feeding-induced mortality in Yellow Fever mosquitoes.

897 Proceedings of the National Academy of Sciences of the United States of America.
898 2011;108(24):E211-7. doi: 10.1073/pnas.1102637108.
899 82. Saldaña MA, Etebari K, Hart CE, Widen SG, Wood TG, Thangamani S, et al.
900 Zika virus alters the microRNA expression profile and elicits an RNAi response in Aedes
901 aegypti mosquitoes. PLoS Neglected Tropical Diseases. 2017;11(7):e0005760-18. doi:
902 10.1371/journal.pntd.0005760.
903 83. Coon KL, Vogel KJ, Brown MR, Strand MR. Mosquitoes rely on their gut
904 microbiota for development. Molecular Ecology. 2014;23(11):2727-39. doi:
905 10.1111/mec.12771.
906
907

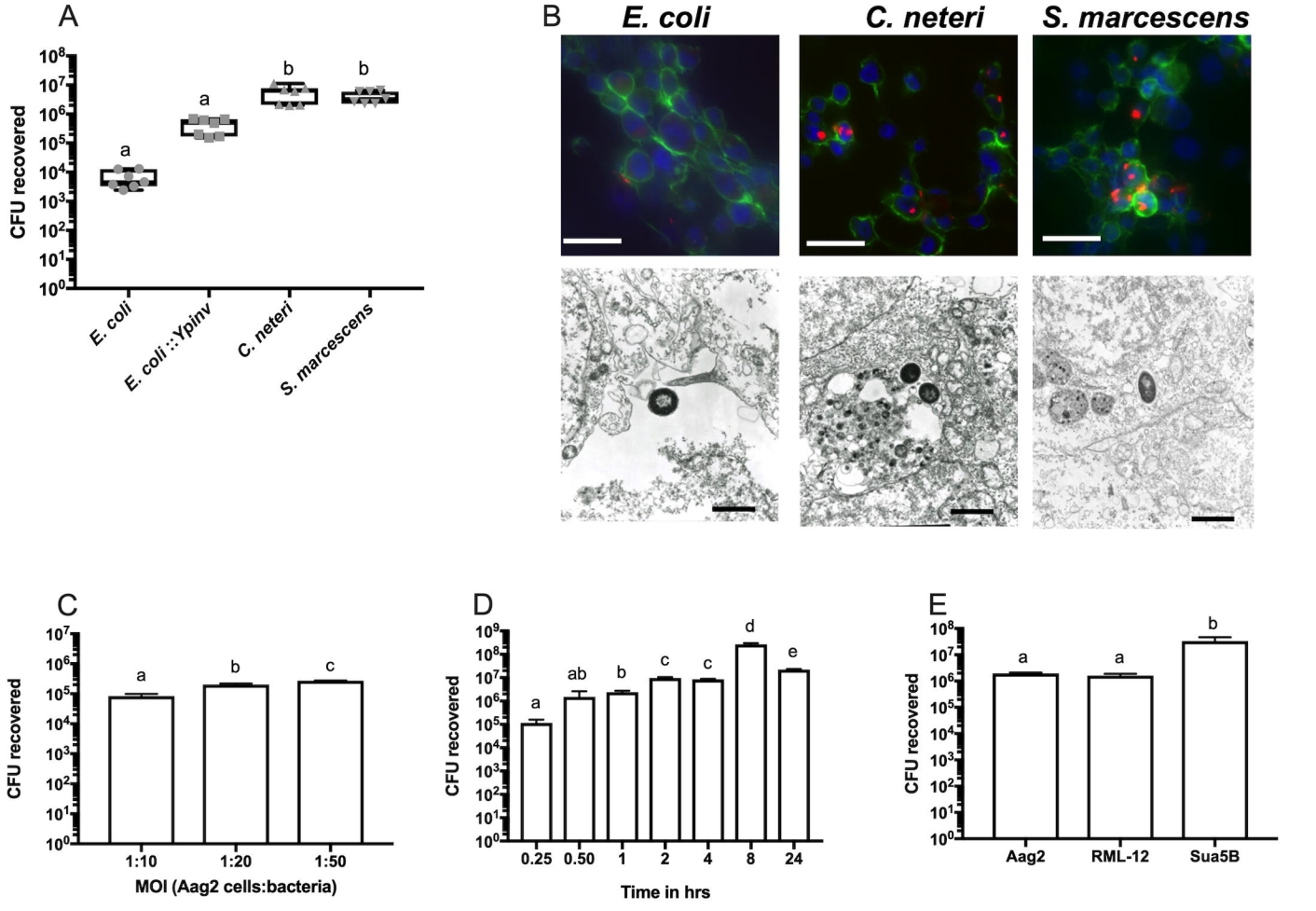
A
CFU recovered
10^8
10^7
10^6
10^5
10^4
10^3
10^2
10^1
10^0
a
a
b
b
E. coli
E. coli ::Ypinv
C. neteri
S. marcescens
B
E. coli
C. neteri
S. marcescens
C
CFU recovered
10^7
10^6
10^5
10^4
10^3
10^2
10^1
10^0
a
b
c
1:10
1:20
1:50
MOI (Aag2 cells:bacteria)
D
CFU recovered
10^9
10^8
10^7
10^6
10^5
10^4
10^3
10^2
10^1
10^0
a
ab
b
c
c
d
e
0.25
0.50
1
2
4
8
24
Time in hrs
E
CFU recovered
10^8
10^7
10^6
10^5
10^4
10^3
10^2
10^1
10^0
a
a
b
Aag2
RML-12
Sua5B

A

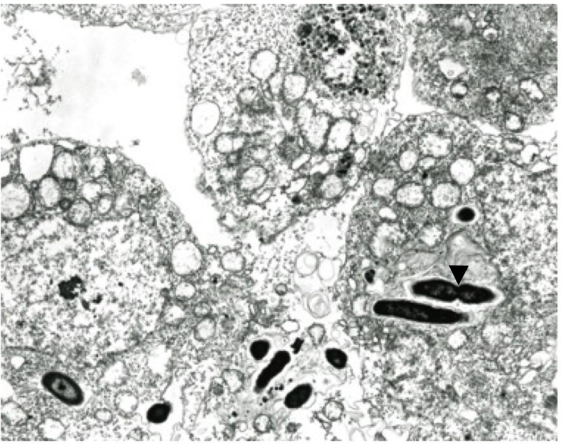

B

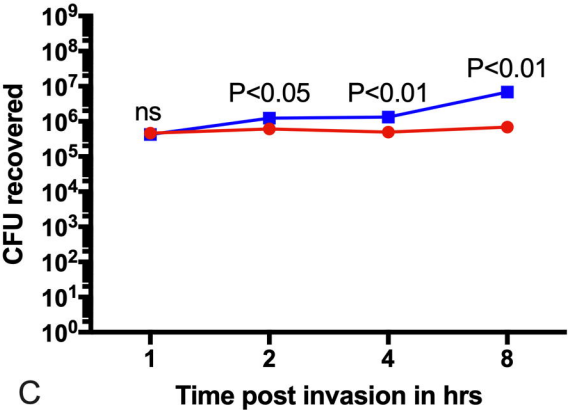
CFU recovered
10^9
10^8
10^7
10^6
10^5
10^4
10^3
10^2
10^1
10^0
ns
P<0.05
P<0.01
P<0.01
1
2
4
8
Time post invasion in hrs

C

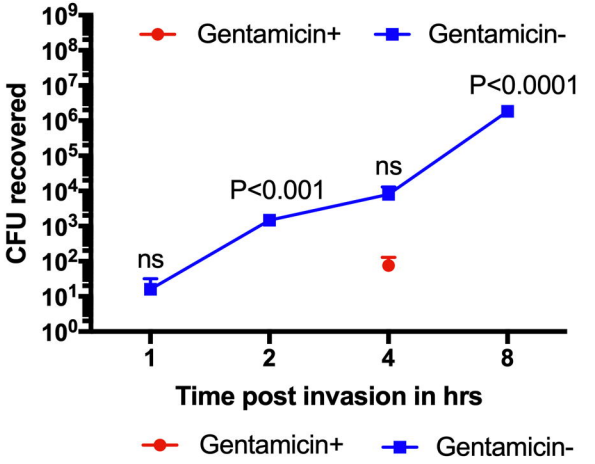
Gentamicin+
Gentamicin-
CFU recovered
10^9
10^8
10^7
10^6
10^5
10^4
10^3
10^2
10^1
10^0
ns
P<0.001
ns
P<0.0001
1
2
4
8
Time post invasion in hrs
Gentamicin+
Gentamicin-

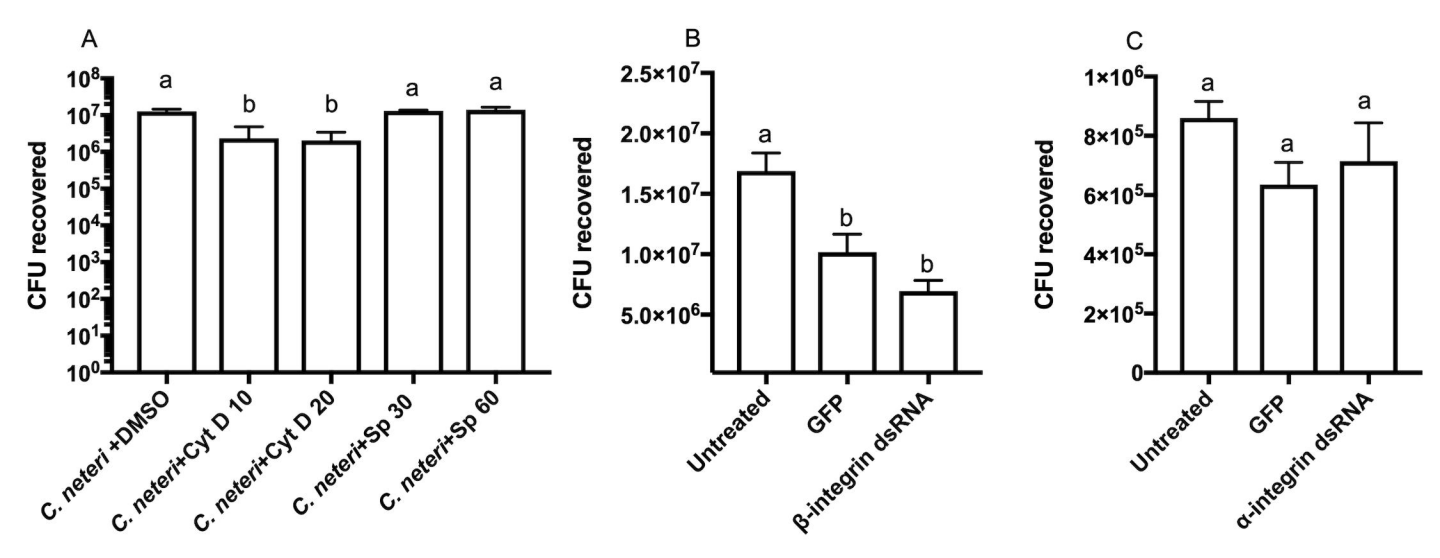
A
CFU recovered
10^8
10^7
10^6
10^5
10^4
10^3
10^2
10^1
10^0
a
b
b
a
a
C. neteri +DMSO
C. neteri+Cyt D 10
C. neteri+Cyt D 20
C. neteri+Sp 30
C. neteri+Sp 60
B
CFU recovered
2.5×10^7
2.0×10^7
1.5×10^7
1.0×10^7
5.0×10^6
a
b
b
Untreated
GFP
β-integrin dsRNA
C
CFU recovered
1×10^6
8×10^5
6×10^5
4×10^5
2×10^5
0
a
a
a
Untreated
GFP
α-integrin dsRNA

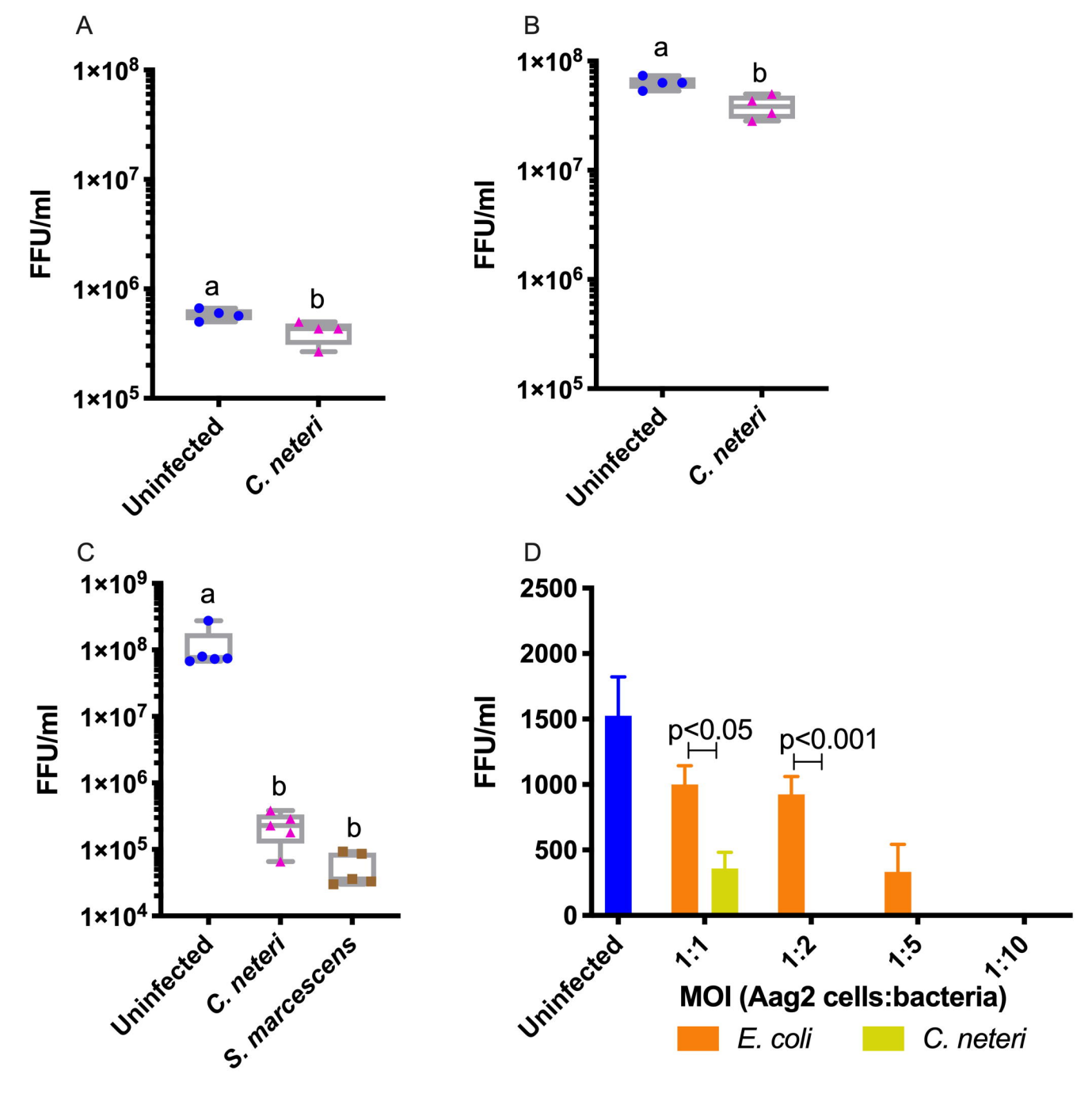
A
1×10^8
1×10^7
1×10^6
1×10^5
FFU/ml
a
b
Uninfected
C. neteri
B
1×10^8
1×10^7
1×10^6
1×10^5
FFU/ml
a
b
Uninfected
C. neteri
C
1×10^9
1×10^8
1×10^7
1×10^6
1×10^5
1×10^4
FFU/ml
a
b
b
Uninfected
C. neteri
S. marcescens
D
2500
2000
1500
1000
500
0
FFU/ml
p<0.05
p<0.001
Uninfected
1:1
1:2
1:5
1:10
MOI (Aag2 cells:bacteria)
E. coli
C. neteri

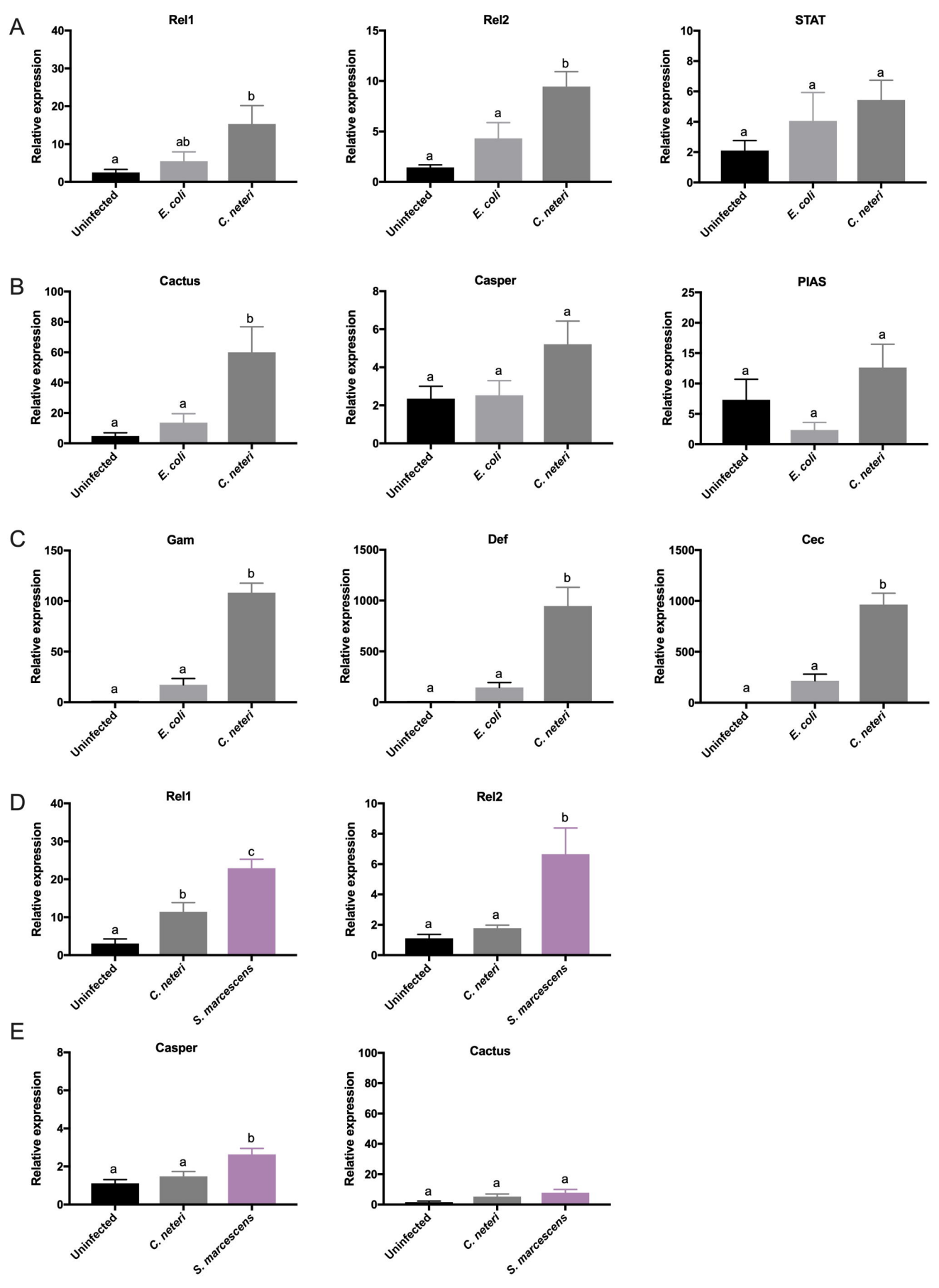
A
Rel1
Relative expression
40
30
20
10
0
a
ab
b
Uninfected
E. coli
C. neteri
Rel2
Relative expression
15
10
5
0
a
a
b
Uninfected
E. coli
C. neteri
STAT
Relative expression
10
8
6
4
2
0
a
a
a
Uninfected
E. coli
C. neteri
B
Cactus
Relative expression
100
80
60
40
20
0
a
a
b
Uninfected
E. coli
C. neteri
Casper
Relative expression
8
6
4
2
0
a
a
a
Uninfected
E. coli
C. neteri
PIAS
Relative expression
25
20
15
10
5
0
a
a
a
Uninfected
E. coli
C. neteri
C
Gam
Relative expression
150
100
50
0
a
a
b
Uninfected
E. coli
C. neteri
Def
Relative expression
1500
1000
500
0
a
a
b
Uninfected
E. coli
C. neteri
Cec
Relative expression
1500
1000
500
0
a
a
b
Uninfected
E. coli
C. neteri
D
Rel1
Relative expression
40
30
20
10
0
a
b
c
Uninfected
C. neteri
S. marcescens
Rel2
Relative expression
10
8
6
4
2
0
a
a
b
Uninfected
C. neteri
S. marcescens
E
Casper
Relative expression
8
6
4
2
0
a
a
b
Uninfected
C. neteri
S. marcescens
Cactus
Relative expression
100
80
60
40
20
0
a
a
a
Uninfected
C. neteri
S. marcescens

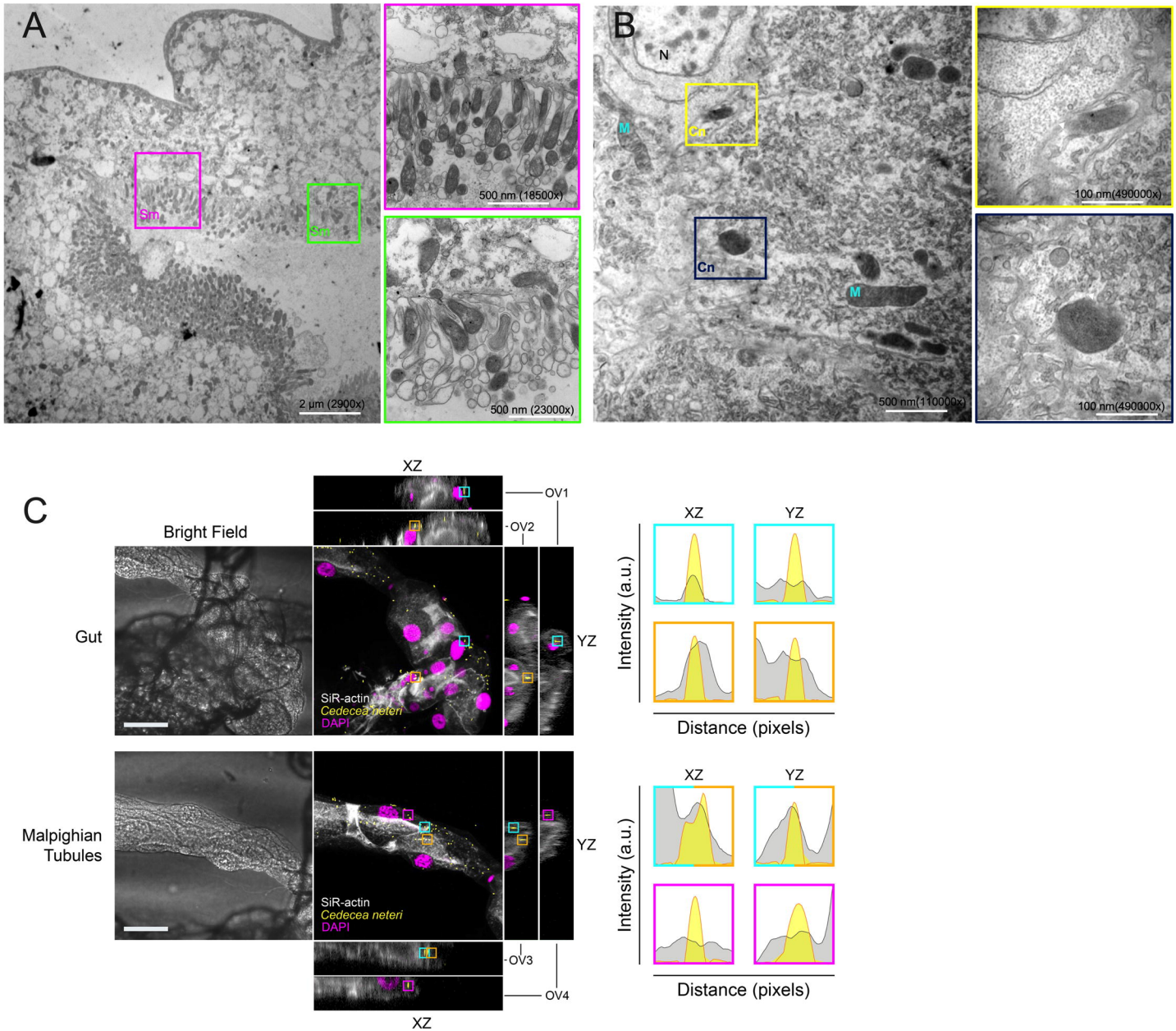
A
Sm
Cn
500 nm (18500x)
500 nm (23000x)
2 µm (2900x)
B
N
M
Cn
Cn
M
100 nm(490000x)
100 nm(490000x)
500 nm(110000x)
C
XZ
OV1
OV2
Bright Field
Gut
YZ
SiR-actin
Cedecea neteri
DAPI
Malpighian Tubules
YZ
SiR-actin
Cedecea neteri
DAPI
OV3
OV4
XZ
XZ
YZ
Intensity (a.u.)
Distance (pixels)
XZ
YZ
Intensity (a.u.)
Distance (pixels)